AGU PUBLICATIONS

Water Resources Research

RESEARCH ARTICLE

Key Points:
- Steady seepage from channel in aquifer with low-permeable substratum is studied
- Seepage losses, phreatic surface and saturated area are computed
- Arbitrary sublayer conductivity and depth, channel width are considered

Supporting Information:
- Supporting Information S1

Correspondence to:
A. R. Kacimov,
anvar@squ.edu.om and
akacimov@gmail.com

An exact analytical solution for steady seepage from a perched Aquifer to a low-permeable sublayer: Kirkham-Brock's legacy revisited

A. R. Kacimov[1] and Yu. V. Obnosov[2]

[1]Department of Soils, Water, and Agricultural Engineering, Sultan Qaboos University, Muscat, Oman, [2]Institute of Mathematics and Mechanics, Kazan Federal University, Kazan, Russia

Abstract An analytical solution is obtained for steady 2-D potential seepage flow from a nonclogged and nonlined soil channel into a highly permeable porous layer, with phreatic surfaces tapering toward a horizontal interface with a subjacent low-permeable formation. Along this boundary, a vertical component of the Darcian velocity vector equals the formation saturated hydraulic conductivity. The image of the physical flow domain in the hodograph plane is a circular polygon, a triangle or digon in a limiting case of a "phreatic jet" impinging on the low-permeable substratum. The polygon is mapped onto an auxiliary half plane, where the complex physical coordinate and complex potential are reconstructed by the Polubarinova-Kochina method, i.e., by solution of a Riemann BVP. The seepage flow rate from the channel, free surfaces, and a saturated (water-logged) area are found for different thicknesses of the top layer, channel widths, and conductivity ratios of the two strata. In particular, the earlier results of Brock, Kirkham, and Youngs, which are based on a numerical solution, Dupuit-Forchheimer (DF) approximation, and approximate potential model, are confirmed in the full 2-D models. Sufficiently far from the channel, the phreatic surface and interface make a wedge. For a sufficiently deep substratum, three zones are analytically distinguished: an almost vertical 1-D descending flow, an almost wedge-configured 1-D flow, and an essentially 2-D zone in between, where neither a standard infiltration theory nor DF analysis are valid.

1. Introduction

In arid Gulf countries, including Oman, managed aquifer recharge (MAR) from ponds, basins, ditches, and other surface impoundments (hereafter called channels) often occurs through a top highly permeable alluvium of conductivity k_1 [*Maliva et al.*, 2014; *Missimer et al.*, 2012], with a subjacent ancient alluvium of a much lower hydraulic conductivity k_2. The dammed rain-born surface runoff or excess tertiary treated water from sewage treatment plants (STP) is seasonally (from several weeks to several months) available for MAR [*Al-Ismaily et al.*, 2013] (see also the photo gallery in the supporting information file). The rest of the year many MAR infiltration ponds are dry, similarly to naturally recharged desert soils and vadose zone, which are replenished through occasionally flowing wadis [see, e.g., *Batlle-Aguilar and Cook*, 2012; *Boisson et al.*, 2014; *Shanafield and Cook*, 2014]. For example, the Haya STP in Oman operates several infiltration ponds (called lagoons), one of which is empty during summer and full in winter. A large "winter" groundwater mound relatively rapidly decays in a subjacent aquifer of high transmissivity [*Kacimov et al.*, 2014]. Other lagoons discharge into a permanently flowing channel (see the photo gallery) but the seepage from this soil (unlined) channel is controlled mostly by the channel stage (transient) and the properties of the soil and substratum rather than the transient groundwater mound.

Because of aridity, the regional water table is often deep (tens and sometimes even hundreds of meters from the ground surface). It does not have enough time to react to the MAR impulse-type infiltration in a Hantush manner, i.e., by forming a gradually rising mound that is commonly expected by MAR engineers, who are used to hydrogeology of humid climates where infiltration from the basin bed is long lasting or even permanent. Instead, a fully saturated ("perched" or "ephemeral") zone ("aquifer") of a limited size is rapidly formed under the MAR surface source, which infiltrates in an intermittent regime (A. R. Kacimov et al., Modeling of transient water table response to MAR: A Lagoon in Muscat, Oman, submitted to *Environmental Earth Science*, 2015). When the MAR stops, this zone vanishes shortly after [*Kacimov et al.*, 2014].
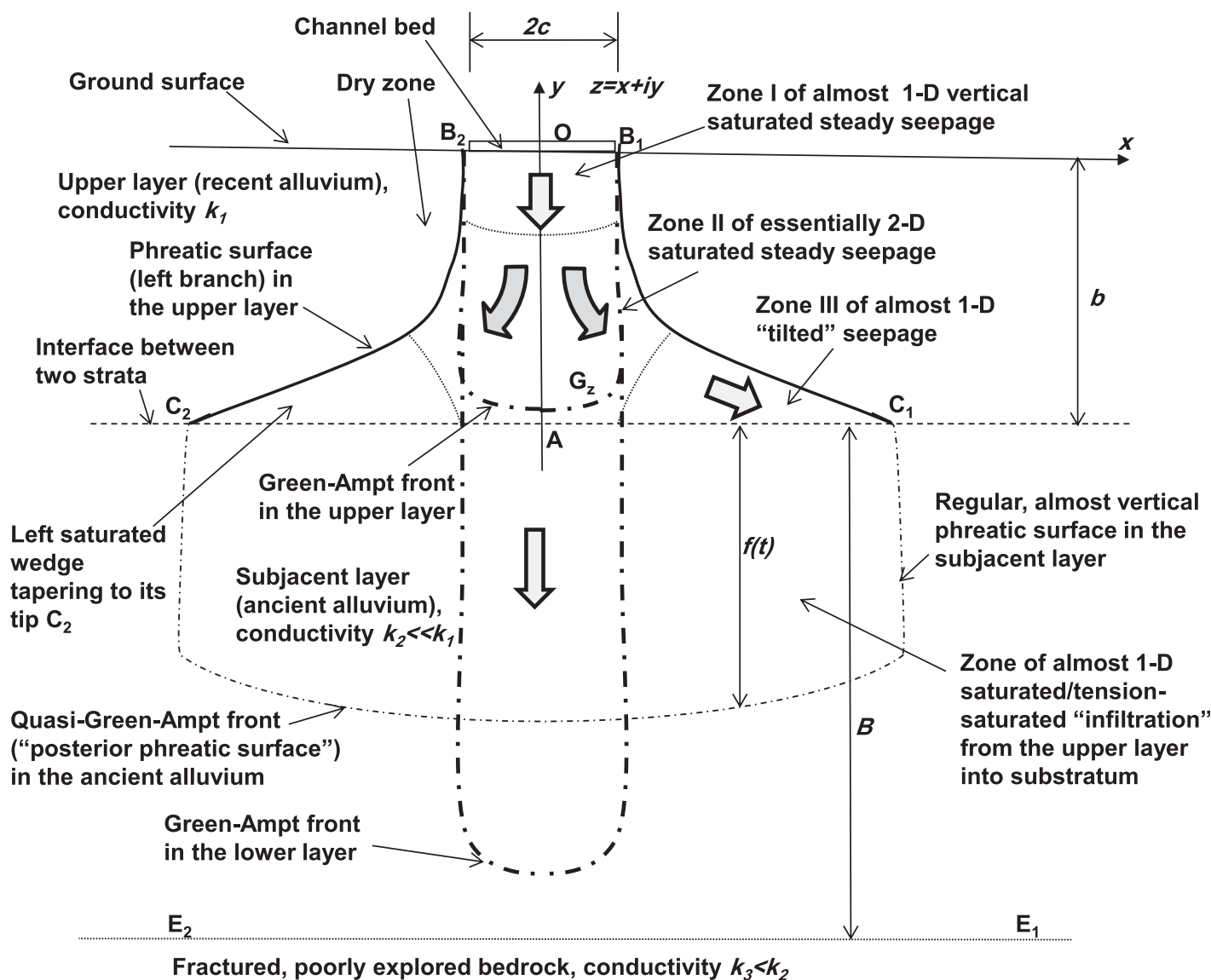
Figure 1. Vertical cross section of flow domain for seepage from a soil channel into a highly permeable layer overlying a low-permeable substratum.

Consequently, there is no "undisturbed," "homeostatic," or "equilibrium" Hantush-type water table to which the MAR-agitated subsurface hydrological system evolves in humid (or deep) aquifers. Figure 1 shows this "perched" MAR entity in a vertical cross section perpendicular to the channel axis, with two "wings" of the MAR plume spread left and right of the channel. Consequently, seepage from the channel is controlled by the channel sizes (width $2c$) and hydraulic/capillary properties of the topmost layers 1 and 2 in Figure 1. Soil physicists dealing with irrigation of layered soils from furrows are well aware of this type of perched zones with saturated "wings" emanating from a channel in a highly permeable soil and tapering toward a low-permeable subsoil [see, e.g., *Brutsaert*, 1971, Figure 4a].

The channel bed B_1OB_2 of width $2c$ (Figure 1) is not clogged and corresponds to Figure 9 of *Bouwer* [2002] and Figure 1a of *Youngs* [1977]. Clogging (also called caking or siltation) of MAR infiltration basins is common [*Bartak et al.*, 2015] if the rapid feeding current upstream of an infiltration basin entrains and carries a load of fine sediments that is common in natural runoff-fed channels [see, e.g., *Al-Ismaily et al.*, 2013]. No-clogging implies that the channel bed is a constant head boundary, while clogged beds require a
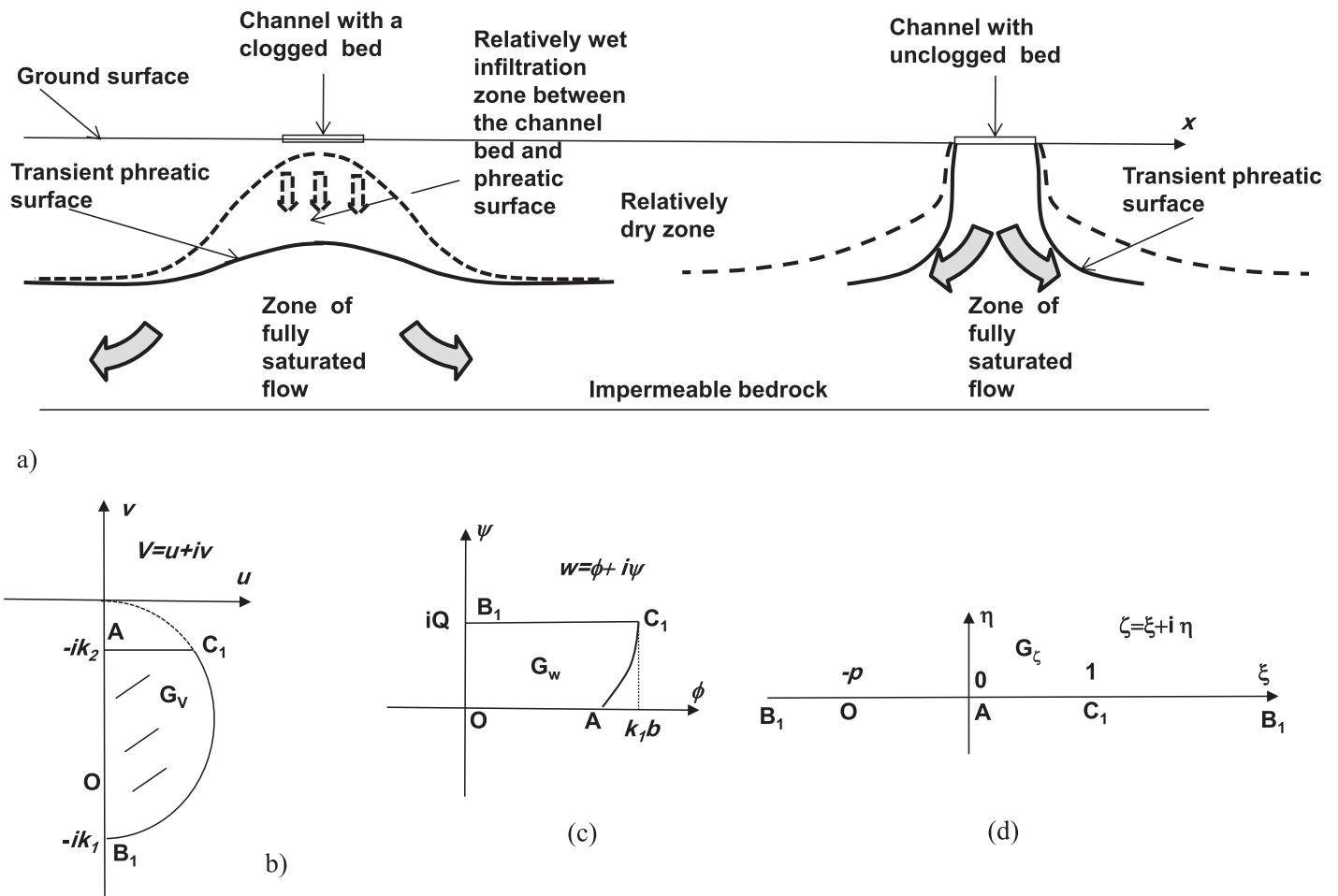
Figure 2. (a) Vertical cross sections for transient *Bouwer* [2002] regimes of infiltration from a clogged and unclogged channel beds into an unconfined aquifer with a subjacent impermeable bedrock; (b) circular triangle in the hodograph corresponding to the right half of the flow domain in the physical plain of Figure 1; (c) complex potential domain; (d) auxiliary half plane.

refraction boundary condition. In case of a low-turbidity tertiary-quaternary water discharged from STPs or water from desalination plants, as an input into the channel, the sediment load is almost nil and the bed remains unclogged. Figure 2a (left and right) illustrates the clogged and unclogged situations. In the former case, there is an unsaturated gap between the channel bed and a bulging groundwater mound (the dashed line illustrates how the phreatic surface rises and the unsaturated zone dwindles). In the latter case, the two branches of the phreatic surface rise faster owing to a direct hydraulic contact between the channel (surface) water and groundwater. *Hantush* [1967] studied axisymmetric transient problems for circular infiltration basins, which are analogous to our case of channels in Figure 2 (left).

Khan et al. [1976, Figure 1] and *Brock* [1982, Figure 1], hereafter abbreviated as **KB**—Kirkham and Brock, considered a MAR regime of a clogged bed such that a strip of a given accretion intensity-fed groundwater mounds with a stable water table. The mounds were hydraulically disconnected from the channel bed (our Figure 2a, left). This regime corresponds to Figure 8 of *Bouwer* [2002]. *Youngs* [1977] considered a homogenous aquifer with an impermeable bottom and studied the transient problem of a mound under an unclogged ditch. **KB** studied actually a two-layered formation with a substratum, although tight but of a finite conductivity.

The main peculiarity of the **KB** model, as compared with the plethora of post-Hantush transient groundwater mound models, is that it has a steady state flow regime. This allowed **KB** to examine a 2-D potential flow governed by the Laplace equation for the hydraulic head and full nonlinear boundary conditions along the water table. **KB** did not average their flow over the vertical coordinate y (our Figure 1). We recall that

Hantush [1967], *Youngs* [1977], and the vast majority of post-Hantush modelers of groundwater mounds adopted the Dupuit-Forchheimer (DF) approximation, i.e., an averaging over the vertical coordinate that resulted in the Boussinesque equation and its linearizations. This made possible application of the juggernaut of integral transforms (e.g., the Laplace and Hankel transforms), the Green function machinery, separation of variables, etc. [see, e.g., *Marino*, 1975]. As *Polubarinova-Kochina* [1962] (hereafter abbreviated as **PK**), pointed out, the DF model may be inadequate for modeling the free-surface dynamics even with relatively minor perturbations of a homeostatic water table. For flow in our Figure 1, the vertical components of the Darcian velocity near the channel are large, such that the DF theory does not work there. However, far away from the channel axis, the "standard" DF approach is applicable.

Hydrogeologically, the **KB** conceptualization of a slightly permeable substratum as a large-size but low-intensity "sink" with respect to seepage from the channel in Figure 1, adopted in this paper, is reasonable. Hydrogeologists know well [see, e.g., *Tromp-van Meerveld et al.*, 2007] that even tight bedrocks are never perfect aquifuges-aquicludes, especially, where catchment-scale groundwater flows are of concern. In the Northern Batina coastal plain of Oman, where MAR sites are designed and constructed, the **KB** two-layered alluvium geology is typical. We note that most post-Hantush models either ignored the permeability of the bedrock or involved the concept of "leaky layer" aquitards. In the latter case, a modified Helmholtz rather than Laplace's equation serves as a governing PDE for a linearized Boussinesq equation in an unconfined aquifer [see, e.g., *Broda et al.*, 2011; *Hemker*, 1984; **PK**]. A "leaky layer" model calls for reliable information on at least three hydrostratigraphic units (two aquifers and an aquitard sandwiched between them), which are "hydraulically connected." This kind of "leaky" connection is common in humid countries like Holland, but is not realized in MAR projects or natural recharge events in shallow soil layers of desert environments. At the MAR sites of Oman, for instance, there is a fractured bedrock (limestone, dolomite and even ophiolite) deep under the second cemented alluvium layer of Figure 1. The wetting front generated by the MAR event may not reach the dotted line ($y = -b-B$) corresponding to the interface between the bedrock and second alluvium layer in Figure 1. The front may also arrive at the bedrock long after seepage from the channel ceases and then there will be no hydraulic contact between the channel and groundwater mound.

In Figure 1, water seeps into the first (main) layer of thickness b (common values in Oman are 2–20 m). Because of a relatively small depth of infiltration basins (common values in Oman are 1–2 m) we assume that the channel in Figure 1 has a negligible depth. Typical values for k_1 and k_2 in Oman are 10–20 and 0.1–2 m/d, respectively. The fractured bedrock at the depth of $B = 200$–600 m (Figure 1, dotted line) is hydraulically hydrogeologically poorly explored as there are almost no pumping tests or tracer experiments in this hydrostratigraphic unit and, consequently, we can ascribe $k_3 = 1$ cm/d for the bedrock. As in **KB**, we assume that the ancient alluvium is infinitely deep and that infiltration into it from a straight horizontal segment C_2AC_1 is at steady state. This may look strange that an "ephemeral" aquifer-mound seeps at steady state, as **KB** conceptualized. However, it can be easily shown that upon commencement of seepage from the channel, a purely vertical flow from the channel bed to the interface between the recent and ancient alluvium in our Figure 1, as qualitatively shown by *Youngs* [1977, Figure 1, dashed lines] and *Gill* [1984, Figure 2, dashed lines] evolves in several hours. After that lateral spreading of the saturated zone to values of L in our Figure 1, necessary for maintaining a steady state regime at typical porosities and recharge rates from the channel, takes place within several days, that can be easily illustrated by either **PK** or *Youngs* [1977] experiments and solutions to the Boussinesq equation with the constant head or constant flux input boundary condition, respectively. We note that *Youngs* [1977] who assumed a constant-seepage rate flow from a ditch, rather than a constant head as in our Figure 1, used *Barenblatt et al.* [1990] analytical 1-D solution to study a transient flow over an impermeable substratum, as shown in our Figure 2a.

Phreatic surfaces B_1C_1 and B_2C_2 in the upper layer demarcate a saturated zone of lateral spreading of the MAR plume. Capillarity of the second layer in Figure 1 is also small and, therefore, it can be easily shown that a transient Green-Ampt (GA) model (see **PK**) of "infiltration" with a front, $f(t)$, propagating from the interface into the ancient alluvium, predicts a fast formation of such steady state "infiltration." This front and almost vertical flaccid phreatic surfaces (three dash-dotted curves in the second layer of Figure 1) is induced and maintained by steady state seepage (we recall, lasting for several weeks–months) from the channel. Despite variation with x of the hydraulic head in the upper layer over the interface segment C_2AC_1, the steady rate of infiltration from this layer into the substratum is constant and equals k_2. This is the basic assumption of **KB**'s model and of the classical GA infiltration model, **PK,** for a "late phase" of infiltration.

Our main goal is the determination of the flow rate from the channel, $2Q$. This is a key MAR parameter. If no impedance from the second layer, i.e., if $b=\infty$ (or $k_2 = k_1$) in Figure 1, then $Q = k_1 c$. The low-permeable layer reduces Q. If $k_2 = 0$, a nontrivial steady seepage over a horizontal impermeable plane from the channel in Figure 1 is not possible, as well as any other flow in either Bouwer's regime. Mathematically, this means that in the limit of large time the phreatic surfaces rise, coincide eventually with the abscissa axis in Figure 2a and flow stops.

Recently, interest has arisen in the characteristic times of transition of one state of an aquifer to another under various hydrologic drives, both natural and man-made [see, e.g., *Currell et al.*, 2015; *Simpson et al.*, 2013]. In the language of the mean action time for flow from unclogged channel in our Figure 2 to reach steady state is infinity and corresponds to stagnant groundwater completely occupying the whole soil layer, similarly to the case of transience of the *Youngs* [1977] flow from a ditch. In practice, this quiescent groundwater state is never reached because if MAR is continuous, the recharged water always finds its vents from the aquifer: evaporation, transpiration, outseeps through topographic depressions, drifting downstream along a mild slope of the bedrock (which is never ideally horizontal as in Hantush's or Youngs' MAR schemes) and downstream discharge into the ocean, or pumping from the mound.

The second characteristic of our interest is the shape of the phreatic surfaces in Figure 1. Although MAR in Oman is intermittent, it has been recently monitored that unexpected water logging of the recent alluvium in Figure 1 spreads far from MAR sources, especially in urban areas where evaporation and agricultural pumping are minimal and the damage to foundations is significant. If MAR water is to be recovered during summer (the period of high demand for irrigation of ornamental plants in Muscat), the location of the pumping wells and their screens should fit well the saturated flow domain, G_z, in Figure 1. Taking into account that what is shown in Figure 1 is only a "temporary steady state," in a planned recovery of the groundwater mound of Figure 1 one should realize that pumping from the second layer in Figure 1a is much more difficult and expensive than from the upper layer and recovery from the fractured rock (third layer in Figure 1) is often technically impossible.

2. Mathematical Model and Analytical Solution

We introduce Cartesian coordinates, xOy, with the origin O coinciding with the midpoint of the channel. In a complex physical plane $z = x + iy$, the flow domain is symmetric with respect to the Oy axis and we study flow in the right half of this domain, G_z. The hydraulic head $h(x,y)$ is a harmonic function in G_z. We introduce a complex potential $w=\phi+i\psi$, where $\phi=-k_1 h$ is the velocity potential and ψ is a stream function. The Darcian velocity, $\vec{V}(x,y)$, obeys $\vec{V}(x,y)=-k\nabla h$. A complex Darcian velocity $V = u + iv$ is defined, where $u(x,y)$ and $v(x,y)$ are the horizontal and vertical components of the velocity vector. The complex function $V(z)$ is antiholomorphic (**PK**) and $w(z)$ is holomorphic.

We count the head from $B_1 O$ where $\phi=0$ and stream function—from OA, along which, $\psi=0$. The **KB** model assumes $v = -k_2$ along AC_1 and therefore $\psi=k_2 x$ along this boundary. Along the phreatic surface, pressure is atmospheric (we neglect capillarity) and therefore $\phi+k_1 y=0$ along $B_1 C_1$. This free boundary is also a streamline $\psi=Q$. At point C_1, whose locus is a part of the solution, the free surface intersects the interface between the two layers and hence $\psi_{C_1}=Q=k_2 L$. The hodograph domain, G_V, corresponding to G_z, is depicted in Figure 2b. In this domain, $B_1 C_1$ is a circular arc of a radius $k_1/2$.

The complex potential domain G_w is shown in Figure 2c. Here the image of AC_1 is an unknown curve and therefore G_w is a curvilinear rectangle. With G_V a circular triangle, we use the **PK** method to solve the stated boundary value problem (BVP) by mapping G_V onto an auxiliary half plane Figure 1d such that the image of point O is $-p$ in this plane. (see Appendix A). We recall that mathematically the method is based on solution of the Riemann problem [*Gakhov*, 1966].

We introduce dimensionless variables $(z^*, b^*, w^*, k^*, L^*, Q^*, S^*) = (z/c, b/c, w/(k_1 c), k_2/k_1, L/c, Q/(ck_1), S/c^2)$ and drop superscripts for the sake of brevity. As an example, we computed two cases of a shallow and a deep upper layer: $b = 1.0$ and $b = 3.0$ (Figures 3 and 4, respectively). The right branches of the water table start from the channel edge $x = 1$, $y = 0$.

In these figures, three phreatic surfaces are shown for $k = 0.1$, 0.2, and 0.4 as solid lines. The dashed line represents the *Brock* [1982] DF approximation for the "tip" of the water table near the point C_1 as the line:
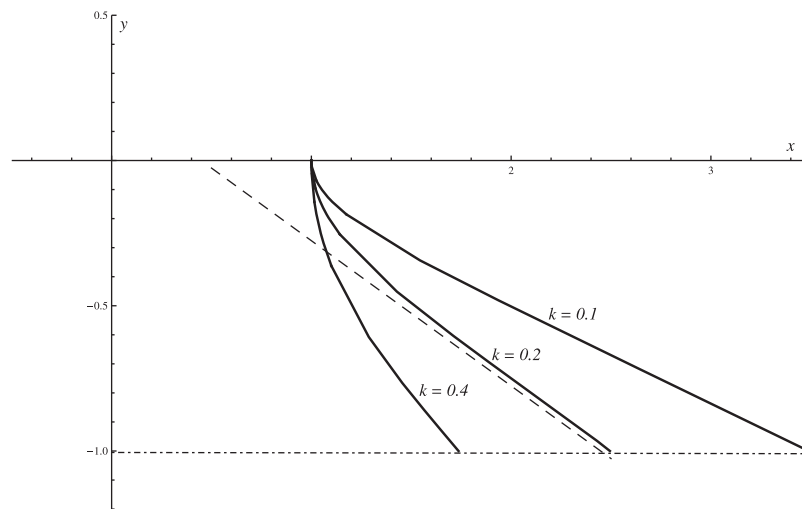
Figure 3. Right branches of the phreatic surface spanning from the channel edge to the leaky substratum for $b = 1$ (solid lines) and the *Brock* asymptotic water table (dashed line).

$$y = \left(\frac{1}{k} - x\right)\sqrt{\frac{k}{1-k}} \tag{1}$$

The dash-dotted line in Figures 3 and 4 indicates the interface. Computations were carried out in *Mathematica* (Wolfram, 1991) using the **ParametricPlot** routine upon integration of the second equation in (A7) and subsequent separation of the real and imaginary parts of $z(\zeta)$ in the interval $1 < \xi < \infty$ that gave $x(\xi)$ and $y(\xi)$, respectively. The parametric equations involved two integrations for which the **NIntegrate** routine of *Mathematica* was used twice. We divided the interval $1 < \xi < \infty$ into three subintervals (each 8–10 points): near point B_1, intermediate, and near point C_1. For each subinterval evaluations in *Mathematica* required about 20 min on a PC Intel Core I7.

Figure 5 shows the conformal mapping parameters p, a, and flow rate Q from a half channel as functions of k spanning from 0.02 to 0.4 and $b = 1$.

As we can see from Figures 3–5, the phreatic surface is indeed close to an oblique asymptote even relatively far from point C_1. The effect of k is strong: for the case shown in Figure 5, Q increases 5 times.
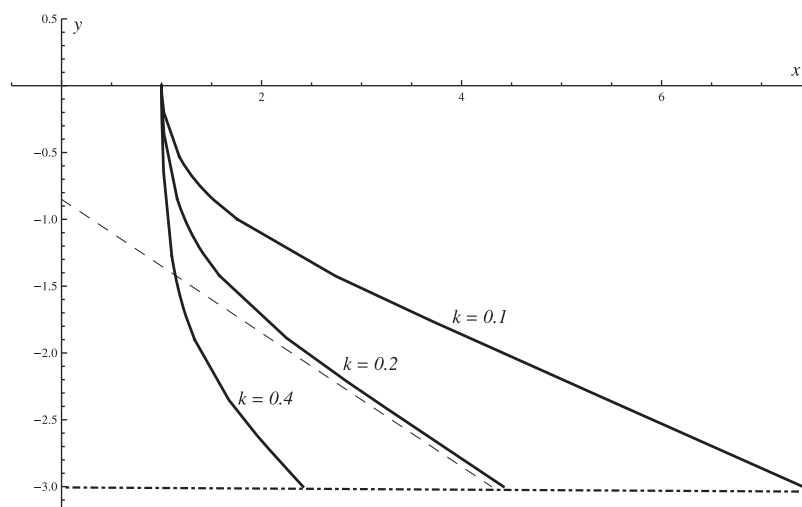
Figure 4. Right branches of the phreatic surface for b = 3 (solid lines) and the *Brock* asymptotic water table (dashed line).
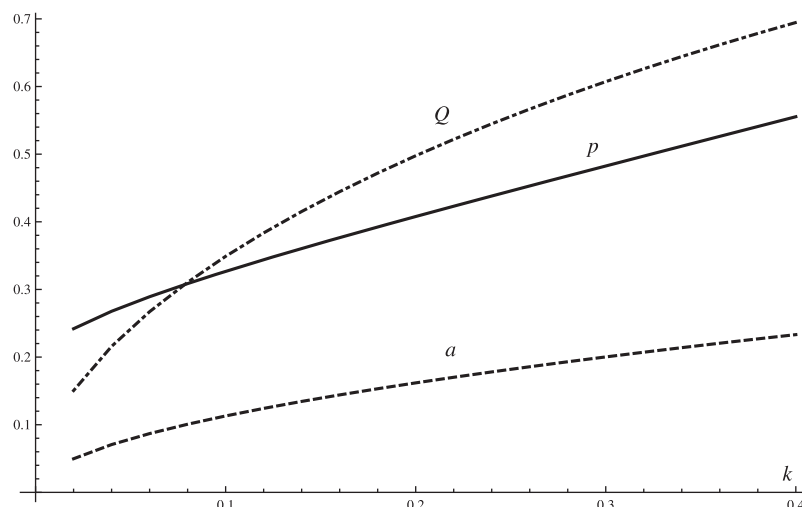
Figure 5. Dimensionless flow rate from a half-channel Q and conformal mapping parameters p and a as functions of dimensionless conductivity of the substratum, k, for $b = 1$.

3. Phreatic Jet Impinging a Low-Permeable Half Plane

As is evident from the previous section and Appendix A, the analytical solution for finite b is cumbersome: it requires mastering the machinery of solving Hilbert's BVP at the level of *Gakhov*'s [1966] book. In this section, we simplify the full seepage problem and obtain an explicit solution for the limit of infinite b in Figure 1, i.e., the case of a very thick upper alluvium (or, returning to dimensional variables, a relatively small channel width c).

We consider a "saturated jet" of width $2c$ descending from infinity and impinging on the interface between two half planes of contrasting conductivities, as shown in Figure 6a. Now points B_1, O, and B_2 of Figure 1 are merged into one point B in Figure 5a and on the Riemann sphere. We shift the origin of Cartesian coordinates to point A in Figure 6a. Then for the whole flow domain G_z of Figure 6a the hodograph domain G_V, shown in Figure 6b, is a digon. We map conformally the domain symmetric with respect to the Ou axis in Figure 6b onto an auxiliary half plane G_ζ in Figure 6c with the correspondence of points $C_1 \to 1$, $C_2 \to -1$, $A \to 0$, $B \to \infty$. The mapping function is [*Koppenfels and Stallman*, 1959]:

$$\frac{dw}{dz}(\varsigma) = \frac{c_1 - \bar{c}_1[(1-\varsigma)/(1+\varsigma)]^\theta}{1 + [(1-\varsigma)/(1+\varsigma)]^\theta} \tag{2}$$

where the branch of the function

$$\chi(\varsigma; \theta) = \left[\frac{1-\zeta}{1+\zeta}\right]^\theta \tag{3}$$

is fixed in the ς-plane with the cut along the segment $[-1, 1]$ by the condition of its positiveness at the upper cut's side;

$$\theta = \frac{1}{2} + \frac{1}{\pi}\arcsin\frac{k_1 - 2k_2}{k_1}, \quad c_1 = \sqrt{k_2(k_1 - k_2)} + ik_2 = i\sqrt{k_1 k_2}e^{-i\pi\theta/2}$$

The fixed branch of the function (3) satisfies the identities

$$\overline{\chi(-\bar{\zeta})} \equiv 1/\chi(\zeta), \qquad \chi(1/\zeta) \equiv e^{-i\pi\alpha/2}\chi(\zeta)$$

The latter identity is true for the upper half of the ζ-plane.

The BVP is formulated as:
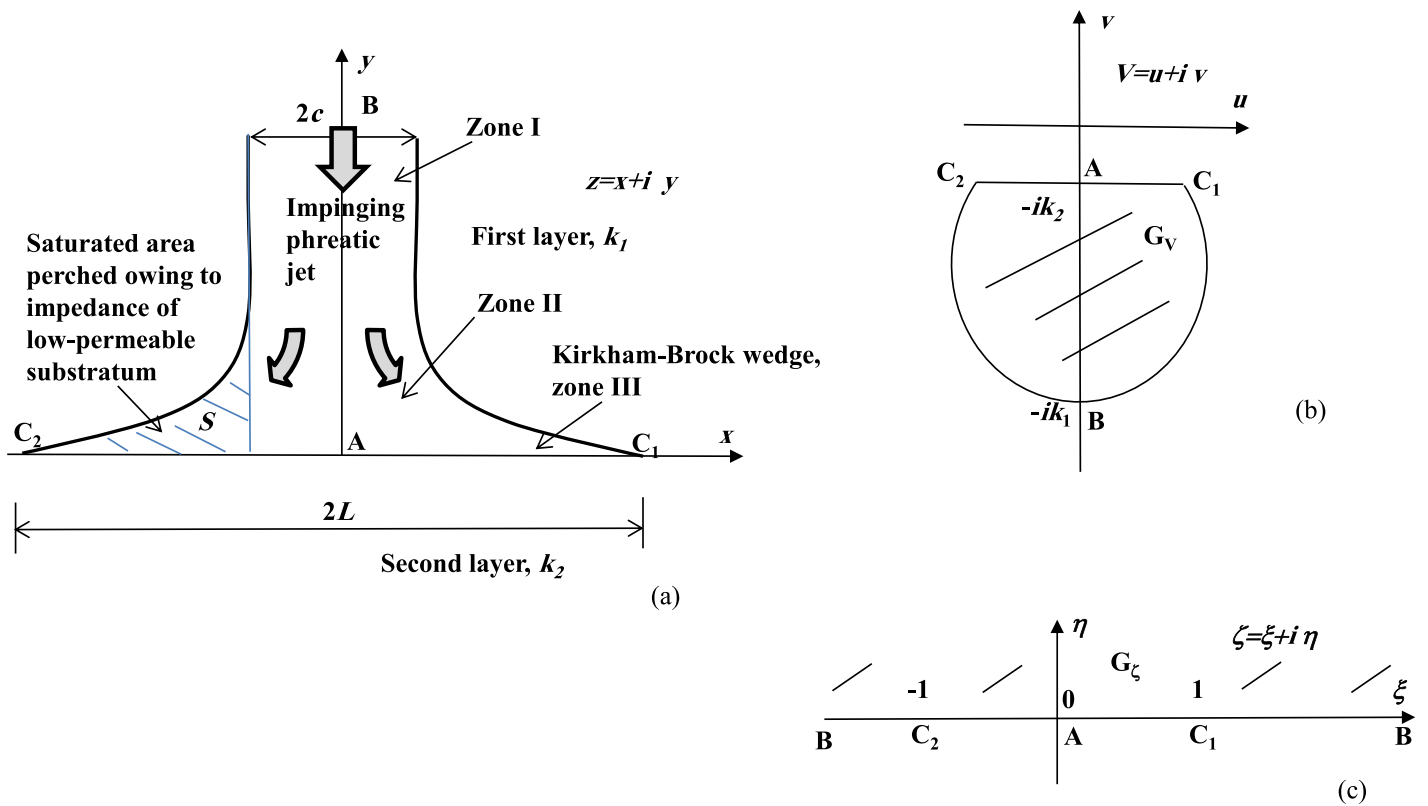
Figure 6. Vertical cross section of a descending phreatic "jet" impinging a low-permeable half plane subjacent to a (a) highly permeable half plane, (b) hodograph digon, and (c) auxiliary half plane.

$$AC_1 : \psi = k_2 x, \quad y = 0$$
$$BC_1 : \psi = Q, \quad \phi + k_1 y = 0 \tag{4}$$
$$BC_2 : \psi = -Q, \quad \phi + k_1 y = 0$$

We recall that at infinity (point B), the complex velocity is $V_1 = -ik_1$. The flow rate through the jet in this problem is known: $2Q = 2Lk_2$ and the spreading width is also known $L = c\, k_1/k_2$.

Solution to BVP (4) is also obtained by the **PK** method (dropped here for the sake of brevity) as:

$$F(\varsigma) = \frac{dw}{d\varsigma} = r\left(\frac{e^{i\pi\alpha/2}\chi(\varsigma;\alpha/2)}{(1-\varsigma)} - \frac{e^{-i\pi\alpha/2}}{(1+\varsigma)\chi(\varsigma;\alpha/2)}\right)$$
$$Z(\varsigma) = \frac{dz}{d\varsigma} = \frac{r}{\sqrt{k_1 k_2}}\left(\frac{\chi(\varsigma;\alpha/2)}{(1-\varsigma)} + \frac{1}{(1+\varsigma)\chi(\varsigma;\alpha/2)}\right). \tag{5}$$

Here $\alpha = 1 - \theta$ and the function $\chi(\varsigma;\alpha/2)$ is defined in (3); $R = \sqrt{k_1/k_2 - 1}$; r is a real constant which has to be found from the condition $\int_{-1}^{1} Z(\xi)d\xi = 2ck_1/k_2$. After simple algebra, $r = ck_1/\pi$.

Equation (5) can be integrated in the first quadrant Re $\zeta > 0$, Im $\zeta > 0$ as

$$w(\varsigma) = ick_1 - \frac{2ck_1}{\pi}\left(e^{i\pi\alpha/2}X(\zeta;\alpha) - e^{-i\pi\alpha/2}X(\zeta;2-\alpha)\right) \tag{6}$$

$$z(\varsigma) = \frac{c}{k} - \frac{2c}{\pi\sqrt{k}}\left((X(\zeta;\alpha) + X(\zeta;2-\alpha))\right) \tag{7}$$

where $w_{C_1} = iQ = ick_1$,
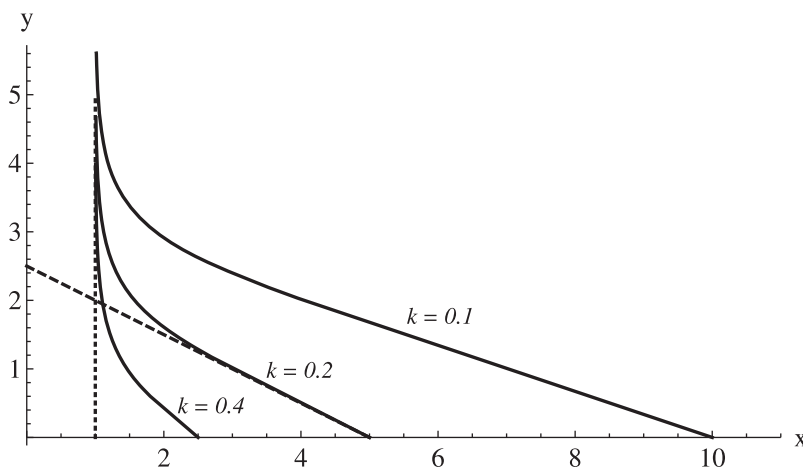
Figure 7. Right branches of the phreatic surface of a phreatic jet (solid lines), the *Brock* asymptotic water table (dashed line), and a vertical phreatic surface for $k = 1$ (dotted line).

$$X(\zeta; \alpha) = \frac{\chi(\zeta; \alpha/2)}{\alpha} F\left(1, \frac{\alpha}{2}; 1 + \frac{\alpha}{2}; \frac{\varsigma - 1}{\varsigma + 1}\right) \quad (8)$$

and $F(a, b; c; \zeta)$ is the hypergeometric function (*Mathematica*'s built-in function **Hypergeometric2F1**).

We note that in the second quadrant of the auxiliary plane Re $\zeta < 0$, Im $\zeta > 0$ our solution is determined by equtions (6–8) in congruity with the symmetry principle for the selected characteristic functions: $w(\zeta) \equiv -\overline{w(-\overline{\zeta})}$, $z(\zeta) \equiv -\overline{z(-\overline{\zeta})}$.

We return to dimensionless variables of the previous section and in Figure 7 present BC_1 for $k = 0.1, 0.2$, and 0.4, plotted by equation (7).

For $k = 0.2$ in Figure 7 the *Brock* [1982] straight line (equation (1)) is shown as a dashed line, which nearly coincides with the free surface at $x > 3$. At $y > 5$ the water table is an almost vertical line $x = 1$ (dotted line). This corroborates the qualitative zonation I–III in Figure 1.

The dimensionless area, S, of the lateral "wings," emerging as an excess of G_z as a saturated half strip in case of $k = 1$, is

$$S(k) = \int_{BC} (x-1)dy = \int_1^\infty [x(\xi) - 1]y'(\xi)d\xi \quad (9)$$

This quantity indicates the upper bound of what is a steady "holding capacity" of the upper alluvium due to the "propping-leaking" action of the ancient alluvium in the original Figure 1. Separating the real and imaginary parts in equation (7), S in equation (9) is evaluated by the **NIntegrate** routine of *Mathematica*. The results are shown in Figure 8. This Figure will be useful if a postinfiltration recovery of groundwater is planned in MAR.

It is evident from Figure 8, that the saturated, and therefore potentially MAR-recoverable area dramatically increases with the decrease of k. Figure 8 presents a means of contrasting the filled region of an aquifer with the quantity of water available from the surface water supply. For example, for the upper reaches of the channel draining the lagoon of Haya company STP typical $c = 1.5$ m and the channel depth is 0.2 m. Therefore, the total quantity of surface water in the channel is 0.3 m³ per 1 m of the channel length. The channel is operated continuously and for the two upper layers in Figure 1 we assessed $k_1 = 10$ m/d, porosity $m_1 = 0.2$ and $b = 50$ m (see Kacimov et al., submitted manuscript, 2015). From the regional hydrostratigraphy, k_2 can be assumed 1 m/d. The low-permeable substratum is so deep that the "impinging jet" regime of Figure 6 is definitely valid. Then from equation (9) $S = 14.32$ (see also Figure 8). Hence, returning to dimensional variable the volume of groundwater stored in both "wings" of the mound is $S_d = 64.5$ m³ per 1 m of the channel length.
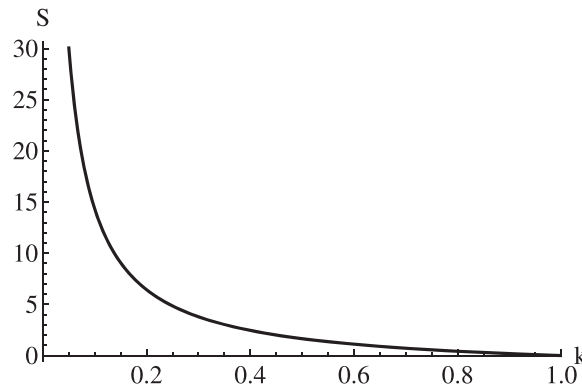
Figure 8. Dimensionless area of one saturated "wing" in Figure 6a.

4. Conclusions

In mathematical models, steady seepage from soil channels is usually [*Bouwer*, 1978; *Gill*, 1984; *Vedernikov*, 1939; **PK**] conceptualized as occurring in a homogeneous soil layer of infinite thickness or a finite-thickness layer with a highly permeable substratum whose interface is a constant head horizon. In the latter case, a horizontal flat water table precedes the MAR event. For finite-thickness, soil layers superjacent of an impermeable strictly horizontal boundary, steady seepage is mathematically not possible and modelers usually specify vertical constant-head discharge lines on the left and right periphery of the flow domain such that water, laterally seeped from the channel and aligned with the impervious horizon, moves into these "vertical drains" [see, e.g., *Bouwer*, 1965; *Wachyan and Rushton*, 1987].

KB realized that absolutely impermeable substrata (bedrocks) are often farfetched assumptions. They pioneered in examining underlying horizons of "tiny permeability" into which the seeped water "infiltrates" from a highly permeable soil layer. Amazingly, the phreatic surface of such "perched aquifers" in nontrivial steady flows is an asymptotic straight line in the vicinity of the intersections between the water table and substratum. In "standard" flow regimes of *Bouwer* [2002] (our Figure 2a) or **PK,** the phreatic surfaces
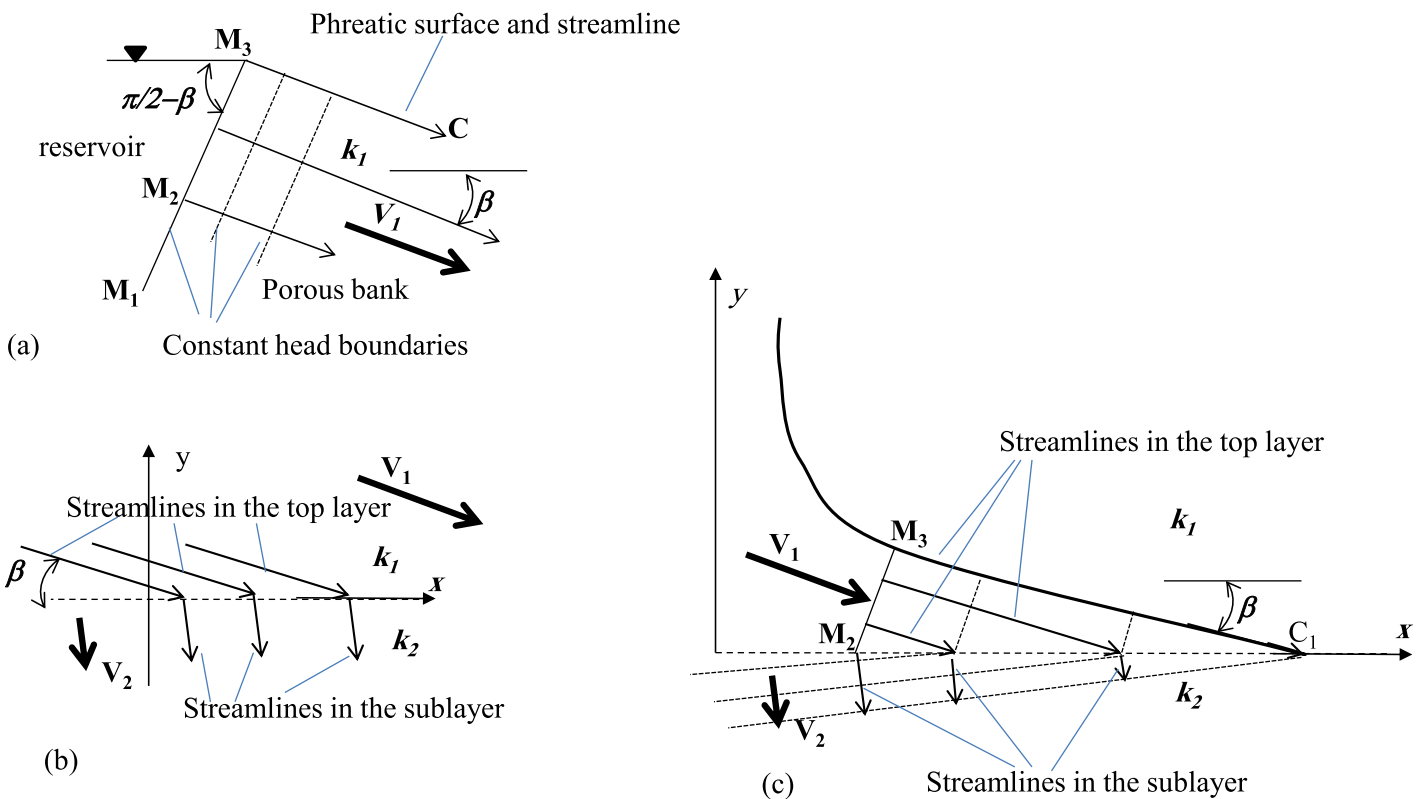
Figure 9. (a) Flow net with ray equipotentials and streamlines for seepage from a reservoir, (b) refraction of an incident unidirectional flow on an interface between two half planes of contrasting conductivity, and (c) refraction problem as adjusted to the wedge zone near point C_1 of Figures 1 and 6a.

emanate from the channel bed and extend to infinity, i.e., the flow domains are not bounded from the left and right of the channel. **KB** assumed that along the interface between two strata the vertical component of the Darcian velocity in the upper layer equals the hydraulic conductivity of the second layer that reflects the late-time asymptotics of the 1-D GA infiltration into this substratum. This conceptualization, does not perfectly describe the refraction conditions, which mathematically require the coincidence of the normal components of velocities in two adjacent porous massifs and a specified jump of the tangential velocity components [*Kacimov and Obnosov*, 2012]. However, for high contrasts of the two conductivities, the vertical flow in the second layer of Figure 1 **KB** used approximate analytical and numerical techniques for finding 2-D fields of the hydraulic head—stream function and phreatic surfaces.

Hillslope hydrologists have recently realized the importance of vertical infiltration into a tight bedrock and the hydrological importance of flow there for soil slope stability and base flow of mountain rivers [see, e.g., *Dusek and Vogel*, 2014; *Hardie et al.*, 2012]. In application to MAR projects, phreatic surface flows have been recently studied for seepage from trenches with two-layered formations similar to our Figure 1 [see, e.g., *Teatini et al.*, 2014] and our results qualitatively concur with modeling by numerical solving of steady state Richards' equation [*Hsieh et al.*, 2010].

In this paper, we used an exact analytical model, without any linearizations of the nonlinear free boundary conditions. A conformal mapping of a circular triangle in the hodograph plane onto an upper half plane of an auxiliary complex variable was employed. Then a BVP for the complex potential and complex physical coordinate was solved using the hodograph and linear differential equations (see **PK** for full details). The method is versatile and allows solving 2-D problems with free boundaries [*Kacimov et al.*, 2006], which are not amenable to analytical treatment by other methods, albeit the constancy of the vertical component of velocity along the interface is only an approximation of the GA model. We obtained expressions of the total seepage losses from the channel, phreatic surfaces and the area of the saturated zone under them through physical parameters, viz., the channel width, height above a low-permeable layer, and hydraulic conductivities of the two layers.

Brock [1982] validated the main assumption of the KB "deep sublayer" model, $v = -k_2$ along C_1C_2, by comparisons with the DF approximation and—in our notations—concluded that for $B/b > 9$–30 this assumption is acceptable. It is noteworthy that a "wedge" tip of the steady flow near C_1 and C_2 in Figure 1 is mathematically identical to the *Youngs*' [1974] wedge, for which water oozes from a flow domain through a seepage face. *Brock* [1982] realized that for a general two-layered system the streamlines are refracted along C_1AC_2 but did not present analytical or numerical solutions showing this refraction in the most rigorous potential theory. Here we show how—similarly to *Kacimov and Obnosov* [2012]—this refraction problem can be assembled for the flow elements near the tips, C_1 and C_2.

First, consider flow from a reservoir of an infinite depth (Figure 9a). A constant-head boundary M_1M_3 makes an angle $\pi - \theta$ with the abscissa axis. All streamlines of this flow are parallel rays, collimated with a straight phreatic surface M_3C which is perpendicular to M_1M_3. All constant head boundaries are rays parallel to the reservoir bed. The Darcian velocity of magnitude $V_1 = k_1 \sin\beta$ is constant in the flow domain. Second, consider two texturally contrasting porous massifs in Figure 9b. The incident flow of velocity $\boldsymbol{V_1}$ is refracted at the abscissa axis (interface) such that in the lower half plane the velocity vector is $\boldsymbol{V_2}$. Now we assume that $\boldsymbol{V_1}$ is generated as in Figure 9a, i.e., the horizontal and vertical components of this vector are $u_1 = k_1 \sin\beta \cos\beta$, $v_1 = k_1 \sin^2\beta$ From the known refraction conditions (see, e.g., **PK**), we get $u_2 = k_2 \sin\beta \cos\beta$, $v_2 = k_1 \sin^2\beta$. The constant head boundaries in the lower half plane are indeed almost parallel to the interface if $k_2 << k_1$. Next, we combine flows in Figures 9a and 9b as shown in Figure 9c. Therefore, flow in Figure 9c incorporates both a steady state phreatic surface, without any linearization or DF averaging, and refraction. The *Youngs* [1974] steady state wedge solution was extended by *Kacimov and Brown* [2014] as an analytic element in a transient problem of a slumping groundwater mound. Similarly, the **KB** wedge, as depleted by a slightly permeable substrate, can be employed in transient problems.

Our new analytical solution for seepage from a channel into a highly permeable layer with a subjacent thick low-permeable substratum can be viewed as a new analytic element of *Strack*'s [1989] arsenal. Indeed, in the standard set of conceptualizations of hydrostratigraphic units and corresponding boundary conditions for the problem of steady seepage from a soil channel [*Bouwer*, 1965; *Vedernikov*, 1939;

PK] water, seeped from the channel, is assumed to drain into a constant-head line (horizontal isobaric substratum, and vertical or horizontal lines, which model rivers, talwegs, or topographic depressions commanded by the channel). In a typical case of a highly permeable horizontal substratum the phreatic surface has a horizontal asymptote. In this paper, the substratum is a line of constant vertical component of velocity and the resulting phreatic surface has an oblique asymptote near the substratum and a vertical one straight under the channel. Thus, the whole flow domain in Figure 1 consists of three zones (demarcated by dotted lines): an almost vertical seepage from the channel two almost unidirectional but tilted flows near the tips C_1 and C_2 and an essentially 2-D flows in between. Only in Zone III of Figure 1 the DF theory works.

Topologically, the "slightly infiltrating" substrate of a highly permeable unconfined aquifer alternates the global features of the seepage flow domain in Figures 1 and 6, converting the "vertical jet" into two wedges.

Appendix A

In this appendix, we solve the flow problem shown in Figure 1. The BVP is:

$$OB_1 : \phi=0, \quad y=0$$

$$OA : \psi=0, \vdots \quad x=0$$

$$AC_1 : \psi=k_2 x, \quad y=-b$$

$$B_1 C_1 : \psi=Q, \quad \phi+k_1 y=0$$

(A1)

To solve this BVP, we map conformally by the function

$$\frac{dw}{dz}(\varsigma)=\omega(\varsigma)=\frac{c_1-\bar{c}_1\left[(1-\sqrt{\varsigma})/(1+\sqrt{\varsigma})\right]^\theta}{1+\left[(1-\sqrt{\varsigma})/(1+\sqrt{\varsigma})\right]^\theta}$$

(A2)

the upper half of the ς-plane G_ς in Figure 2d onto the circular triangle G_V^S symmetric with G_V with respect to the real axis. The unknown locus of the point O in the ς-plane is $-p$ ($0 < p < \infty$). This constant (called affix; see **PK**) will be determined later as a part of solution. Determination of affixes for BVPs like (A1) is a daunting problem. **PK** effectively solved the problem for the case of three so-called characteristic points, i.e., the points where the type of the boundary conditions in BVP changes. In our case, the number of these points (shown in Figure 2d) is four.

From equation (A1) and the relation $F(\varsigma)=\omega(\varsigma)Z(\varsigma)$, we get the following Riemann BVP (see *Gakhov* [1966] on the general theory of this problem) for $F(\varsigma)$:

$$OB_1 : \operatorname{Im}(iF(\xi))=0$$

$$OA : \operatorname{Im} F(\xi)=0$$

$$AC_1 : \operatorname{Im}(F(\xi/\omega(\xi))=0$$

$$B_1 C_1 : \operatorname{Im} F(\xi=0$$

(A3)

We use the notations: $F^+(\varsigma)=F(\varsigma)$ for $\operatorname{Im}\varsigma > 0$, and $F^-(\varsigma)=\overline{F(\bar\varsigma)}$ for $\operatorname{Im}\varsigma < 0$. Then, the BVP (A3) is reduced to the Hilbert problem [see *Gakhov*, 1966]:

$$OB_1 : F^+(\xi)=-F^-(\xi)$$

$$OA : F^+(\xi)=F^-(\xi)$$

$$AC_1 : F^+(\xi)=\frac{\omega(\xi)}{\overline{\omega(\xi)}}F^-(\xi)=\frac{\omega(\xi)}{\omega(\xi)-2ik_2}F^-(\xi)$$

$$B_1 C_1 : F^+(\xi)=F^-(\xi)$$

(A4)

We use an arbitrary branch of the function $\sqrt{\varsigma+p}$, fixed in the ς-plane with a cut along the ray $(-\infty, -p)$ and introduce the function

$$\Phi(\varsigma) = \frac{1}{\sqrt{\varsigma + p}} \begin{cases} F^+(\varsigma), & \operatorname{Im}\varsigma > 0 \\ F^-(\varsigma), & \operatorname{Im}\varsigma < 0 \end{cases}$$

which is holomorphic everywhere in the ς-plane with a cut along the segment $[0, 1]$, except the point $\varsigma = -p$ where $\Phi(\varsigma)$ has a simple pole because the complex potential $w(\varsigma)$ at points $-p$ and at infinity has the following behavior:

$$w(\varsigma) \propto \mathrm{O}(\sqrt{\varsigma + p}), \qquad w(\varsigma) - iQ \propto \mathrm{O}(1/\sqrt{\varsigma})$$

correspondingly (see Figures 2c and 2d). Therefore, in the vicinity of these points, we have the following behavior:

$$Z(\varsigma) = \frac{dz}{d\varsigma} \propto \mathrm{O}\left(\frac{1}{\sqrt{\varsigma + p}}\right), \qquad F(\varsigma) = \frac{dw}{d\varsigma} \propto \mathrm{O}(\varsigma^{-3/2})$$

Also, $\Phi(\varsigma)$ has a zero of the second order at infinity. The points $\varsigma = 0$ and $\varsigma = 1$ are integrable singular point. For this new function, we get a Hilbert BVP [*Gakhov*, 1966]

$$\Phi^+(\xi) = \Phi^-(\xi)/\Omega(\xi), \quad 0 < \xi < 1$$

It is well known that the Hilbert BVP is one of the 23 famous centennial mathematical problems formulated by David Hilbert in 1900. A general solution of a multidimensional Hilbert BVP is unknown. **PK** obtained solution for few special cases of a two-dimensional characteristic vector function with application to Darcian flows.

We introduce the function

$$\Omega(\varsigma) = \frac{\omega(\varsigma) - 2ik_2}{\omega(\varsigma)} = \frac{\bar{c}_1 - c_1 \left[(1 - \sqrt{\varsigma})/(1 + \sqrt{\varsigma})\right]^\theta}{c_1 - \bar{c}_1 \left[(1 - \sqrt{\varsigma})/(1 + \sqrt{\varsigma})\right]^\theta} = -\frac{1 + e^{-i\pi\theta}\left[(1 - \sqrt{\varsigma})/(1 + \sqrt{\varsigma})\right]^\theta}{e^{-i\pi\theta} + \left[(1 - \sqrt{\varsigma})/(1 + \sqrt{\varsigma})\right]^\theta} \tag{A5}$$

It is holomorphic in the upper half of the ς-plane. $\Omega(\varsigma)$ maps conformally this half plane onto the domain defined by the inequalities $|\Omega| < 1$, $\operatorname{Im}\Omega < 0$, $\operatorname{Re}\Omega < 1 - 2k$. This function can be analytically continued by the symmetry principle into the lower half of the ς-plane through any part of the real axis: $(-\infty, 0)$, $(0, 1)$, or $(1, \infty)$.

We introduce the function

$$\chi(\varsigma) = \exp\left\{-\frac{1}{2\pi i} \int_0^1 \log\Omega(t)\frac{dt}{t - \varsigma}\right\} = \exp\left\{-\frac{1}{2\pi} \int_0^1 Arg\,\Omega(t)\frac{dt}{t - \varsigma}\right\} \tag{A6}$$

which factorizes the coefficient $1/\Omega(\xi)$. Then we get

$$\Phi^+(\xi)/\chi^+(\xi) = \Phi^-(\xi)/\chi^-(\xi), \quad -\infty < \xi < \infty$$

Hence, the function $\Phi(\varsigma)/\chi(\varsigma)$ is holomorphic everywhere in the ς-plane, except simple poles at the points $\varsigma = -p$, $\varsigma = 1$. This function has an integrable (and hence removable) singularity at the origin and a second-order zero at infinity. Therefore, due to Liouville's theorem,

$$\Phi(\varsigma) = \frac{a\chi(\varsigma)}{(1 - \varsigma)(\varsigma + p)}$$

where a is an arbitrary real parameter.

Consequently, the required solution is

$$F(\varsigma) = \exp\left\{-\frac{1}{2\pi i} \int_0^1 \log\Omega(t)\frac{dt}{t - \varsigma}\right\}\frac{a}{(1 - \varsigma)\sqrt{\varsigma + p}}, \quad Z(\varsigma) = F(\varsigma)/\omega(\varsigma) \tag{A7}$$

Here both unknown parameters a and p should be evaluated from the given depth of the substratum and half width of the channel in Figure 1. This gives the system

$$\int_0^{-p} Z(t)dt = ib, \qquad \int_{-\infty}^{-p} Z(t)dt = -c$$

or equivalently

$$a\int_{-p}^0 \exp\left\{ -\frac{1}{2\pi}\int_0^1 \arg\Omega(\xi)\frac{d\xi}{\xi-t} \right\} \frac{|\omega(t)|^{-1}}{(1-t)\sqrt{t+p}}dt = b,$$

$$a\int_{-\infty}^{-p} \exp\left\{ -\frac{1}{2\pi}\int_0^1 \arg\Omega(\xi)\frac{d\xi}{\xi-t} \right\} \frac{|\omega(t)|^{-1}}{(1-t)\sqrt{|t+p|}}dt = c$$

(A8)

From equation (A8) we arrive at a nonlinear equation with respect to the affix p:

$$\frac{\int_{-p}^0 \exp\left\{ -\frac{1}{2\pi}\int_0^1 \arg\Omega(\xi)\frac{d\xi}{\xi-t} \right\} \frac{|\omega(t)|^{-1}}{(1-t)\sqrt{t+p}}dt}{\int_{-\infty}^{-p} \exp\left\{ -\frac{1}{2\pi}\int_0^1 \arg\Omega(\xi)\frac{d\xi}{\xi-t} \right\} \frac{|\omega(t)|^{-1}}{(1-t)\sqrt{|t+p|}}dt} = b/c$$

(A9)

For a given pair of values of b and c, we used the **FindRoot** routine of *Mathematica* to evaluate p from equation (A9), where the integrals were computed by the **NIntegrate** routine. Then we calculated the constant a from equation (A8). Eventually, from equations (A7) and (A2), we found the phreatic surface and from $Q = k_2 L$ – half of the seepage losses from the channel.

References

Al-Ismaily, S. S., A. K. Al-Maktoumi, A. R. Kacimov, S. M. Al-Saqri, H. A. Al-Busaidi, and M. H. Al-Haddabi (2013), A morphed block-crack preferential sedimentation: A smart design and evolution in nature, *Hydrol. Sci. J.*, *58*(8), 1779–1788, doi:10.1080/02626667.2013.838002.

Barenblatt, G. I., V. M. Entov, and V. M. Ryzhik (1990), *Flow of Fluids Through Natural Rocks*, Kluwer Acad., Dordrecht, Netherlands.

Bartak, R., T. Grischek, and D. Hoche (2015), MAR with untreated river water: Clogging of basins and coliform removal rates, *J. Hydrol. Eng.*, *20*, B4014001-1-B4014001-6.

Battle-Aguilar, J., and P. G. Cook (2012), Transient infiltration from ephemeral streams: A field experiment at the reach scale, *Water Resour. Res.*, *48*, W11518, doi:10.1029/2012WR012009.

Boisson, A., et al. (2014), Questioning the impact and sustainability of percolation tanks as aquifer recharge structures in semi-arid crystalline context, *Environ. Earth Sci.*, doi:10.1007/s12665-014-3229-2.

Bouwer, H. (1965), Theoretical aspects of seepage from open channels, *J. Hydraul. Div. Am. Soc. Civ. Eng.*, *91*(HY3), 37–59.

Bouwer, H. (1978), *Groundwater Hydrology*, McGraw-Hill, N. Y.

Bouwer, H. (2002), Artificial recharge of groundwater: Hydrogeology and engineering, *Hydrogeol. J.*, *10*, 121–142.

Brock, R. (1982), Steady state perched groundwater mounds on thick sublayers, *Water Resour. Res.*, *18*(2), 376–382.

Broda, S., C. Paniconi, and M. Larocque (2011), Numerical investigation of leakage in sloping aquifers, *J. Hydrol.*, *409*, 49–61.

Brutsaert, W. F. (1971), A functional iteration technique for solving the Richards equation applied to two-dimensional filtration problems, *Water Resour. Res.*, *7*(6), 1583–1596.

Currell, M., T. Gleeson, and P. Dahlhaus (2015), A new assessment framework for transience in hydrogeological systems, *Groundwater*, doi:10.1111/gwat.12300, in press.

Dusek, J., and T. Vogel (2014), Modeling subsurface hillslope runoff dominated by preferential flow: One-vs. two-dimensional approximation, *Vadose Zone J.*, *13*(6), doi:10.2136/vzj2013.05.0082. [Available at http://vzj.geoscienceworld.org/content/13/6/vzj2013.05.0082.full.]

Gakhov, F. D. (1966), *Boundary Value Problems*, Pergamon, Oxford, U. K.

Gill, M. A. (1984), Water table rise due to infiltration from canals, *J. Hydrol.*, *70*, 337–352.

Hantush, M. S. (1967), Growth and decay groundwater-mound in response to uniform percolation, *Water Resour. Res.*, *1*(3), 227–234.

Hardie, M. A., R. B. Doyle, W. E. Cotching, and S. Lisson (2012), Subsurface lateral flow in texture-contrast (Duplex) soils and catchments with shallow bedrock, *Appl. Environ. Soil Sci.*, 2012, *10*, doi:10.1155/2012/861358.

Hemker, C. J. (1984), Steady groundwater flow in leaky multiple aquifer systems, *J. Hydrol.*, *72*, 355–374.

Hsieh, H. H., C. H. Lee, C. S. Ting, and J. W. Chen (2010), Infiltration mechanism simulation of artificial groundwater recharge: A case study at Pingtung Plain, Taiwan, *Environ. Earth Sci.*, *60*, 1353–1360, doi:10.1007/s12665-009-0194-2.

Kacimov, A. R., and G. Brown (2014), A transient phreatic surface mound, evidenced by a strip of vegetation in an earth dam shoulder: The Lembke-Youngs reductionist model revisited, *Hydrol. Sci. J.*, *60*(2), 361–378, doi:10.1080/02626667.2014.913793.

Kacimov, A. R., and Yu. V. Obnosov (2012), Analytical solutions for seepage near material boundaries in dam cores: The Davison-Kalinin problems revisited, *Appl. Math. Modell.*, *36*, 1286–1301, doi:10.1016/j.apm.2011.07.088.

Kacimov, A. R., Yu. V. Obnosov, M. M. Sherif, and J. Perret (2006), Analytical solution to a sea water intrusion problem with a fresh water zone tapering to a triple point, *J. Eng. Math.*, *54*(3), 197–210, doi:10.1007/s10665-006-9030-9.

Kacimov, A. R., V. Zlotnik, and A. Al-Maktoumi (2014), Analytical model of aquifer response to artificial groundwater recharge from Wadi channels, in *10th International Hydrogeological Congress of Greece, 8–10 October 2014, Thessaloniki, Greece*, vol. 1, edited by K. Voudoris et al., pp.259–267, Geol. Soc. of Greece, Thessaloniki, Greece.

Khan, M. Y., D. Kirkham, and R. L. Hardy (1976), Shapes of steady state perched groundwater mounds, *Water Resour. Res.*, *12*(3), 429–436.

Koppenfels, F., and S. Stallman (1959), *Praxis der Konformen Abbildung*, Springer, Berlin.

Maliva, R. G., R. Herrmann, K. Coulibaly, and W. Guo (2014), Advanced aquifer characterization for optimization of managed aquifer recharge, *Environ. Earth Sci.*, doi:10.1007/s12665-014-3167-z.

Marino, M. A. (1975), Artificial groundwater recharge, I. Circular recharging area, *J. Hydrol.*, *25*, 201–208.

Missimer, T. M., J. E. Drewes, G. Amy, R. G. Maliva, and S. Keller (2012), Restoration of Wadi aquifers by artificial recharge with treated waste water, *Ground Water*, *50*(4), 514–527.

Polubarinova-Kochina, P. Ya. (1962), *Theory of Ground Water Movement*, Princeton Univ. Press, Princeton, N. J. [Second edition, in Russian, Nauka, Moscow, 1977]

Shanafield, M., and P. G. Cook (2014), Transmission losses, infiltration and groundwater recharge through ephemeral and intermittent streambeds: A review of applied methods, *J. Hydrol.*, *511*, 518–529.

Simpson, M. J., F. Jazaei, and T. P. Clement (2013), How long does it take for aquifer recharge or aquifer discharge processes to reach steady state?, *J. Hydrol.*, *501*, 241–248.

Strack, O. D. L. (1989), *Groundwater Mechanics*, Prentice Hall, Englewood Cliffs, J. W.

Teatini, P., A. Comerlati, T. Carvalho, A.-Z. Gütz, A. Affatato, L. Baradello, F. Accaino, D. Nieto, G. Martelli, G. Granati, and G. Paiero (2014), Artificial recharge of the phreatic aquifer in the upper Friuli plain, Italy, by a large infiltration basin, *Environ. Earth Sci.*, *73*(6), 2579–2593, doi:10.1007/s12665-014-3207-8.

Tromp-van Meerveld, H. J., N. E. Peters, and J. J. McDonnell (2007), Effect of bedrock permeability on subsurface stormflow and the water balance of a trenched hillslope at the Panola Mountain Research Watershed, Georgia, USA, *Hydrol. Processes*, *21*, 750–769.

Vedernikov, V. V. (1939), *Theory of Seepage and Its Applications to Problems of Irrigation and Drainage [in Russian]*, Gosstroiizdat, Moscow.

Wachyan, E., and K. R. Rushton (1987), Water losses from irrigation canals, *J. Hydrol.*, *92*, 275–288.

Wolfram, S. (1991), *Mathematica. A System for Doing Mathematics by Computer*, Addison-Wesley, Redwood City, Calif.

Youngs, E. G. (1974), Seepage rates and the horizontal flow approximation, *Water Resour. Res.*, *10*(4), 874–876.

Youngs, E. G. (1977), The unsteady groundwater mound below an irrigation ditch or leaky canal, *J. Hydrol.*, *34*, 307–314.